Electronic Supplementary Information (ESI)

"Carbolong" Polymers with Near Infrared Triggered, Spatially Resolved and Rapid Self-Healing Property

Huan Zhang,[a,‡] *Haibo Zhao,*[a,b,‡] *Kaiyue Zhu,* [a,b] *Jiangxi Chen,*[c] *Xumin He,*[a,b,]* *Wengui Weng,*[a,]* *and Haiping Xia* [a,b,]*.

[a]Department of Chemistry, College of Chemistry and Chemical Engineering, Xiamen University, Xiamen 361005, China

[b]State Key Laboratory of Physical Chemistry of Solid Surfaces and Collaborative Innovation Center of Chemistry for Energy Materials (iChEM), Xiamen University, Xiamen 361005, China

[c]Department of Materials Science and Engineering, College of Materials, Xiamen University, Xiamen 361005, China

KEYWORDS: metallopolymer, carbolong, photothermal, near infrared, self-healing

*Email: hejin@xmu.edu.cn, wgweng@xmu.edu.cn, hpxia@xmu.edu.cn

Table of Contents

Figures

Tables

Materials and Synthesis

Materials

All reagents, chemicals, materials and solvents were obtained from Sinopharm, Sigma-Aldrich and Aladdin, and used as received unless otherwise noted. poly(ε-caprolactone) (PCL, M_n = 2000 kDa) was dried at 90 °C under vacuum for 3 h before use. DMF was distilled under N_2 over CaH_2 prior to use. All reactions were performed under N_2 atmosphere unless otherwise specified and all glassware was flame dried under vacuum before use.

General Methods

NMR spectroscopic experiments were performed on a Bruker AVIII-500 (^{1}H, 600.1 MHz; ^{13}C, 150.9 MHz; ^{31}P, 242.9 MHz) spectrometer at room temperature. ^{1}H and ^{13}C NMR chemical shifts are relative to tetramethylsilane, and ^{31}P NMR chemical shifts are relative to 85% H_3PO_4. HRMS experiments were conducted on a Bruker En Apex Ultra 7.0T FT-MS. Single-Crystal X-ray diffraction data were collected at 100 K on a XtaLAB Synergy Dualflex HyPix area detector using Cu Kα radiation (λ = 1.54184 Å).

Synthesis and Polymerization

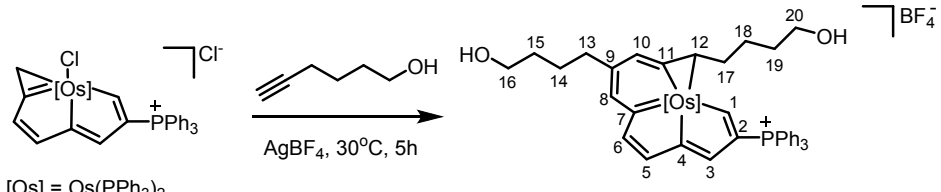

12C-carbolong Complex 2. Complex 1 was synthesized and characterized according previous published route.[1]

hex-5-yn-1-ol (496μL, 4.5 mmol, 5 eq) was added to a mixture of complex **1** (1000 mg, 0.9 mmol, 1 eq) and $AgBF_4$ (526 mg, 2.7 mmol, 3 eq) in dichloromethane (20 mL). The reaction mixture was stirred at 30 °C for 5h to yield a green solution, and then the solid suspension was removed by filtration. The filtrate was reduced under vacuum to approximately 2 mL, and then purified by column chromatography (neutral alumina, eluent: dichloromethane/methanol = 5:1) to give a green solution. The green solid of complex 2 (831 mg, 68 %) was collected after the solvent was evaporated to dryness under vacuum and the resulting residue was washed with diethyl ether and then dried under vacuum.^{1}H NMR plus ^{1}H-^{13}C HSQC (600.1 MHz, CD_2Cl_2): δ = 13.40 (d, $J_{P\text{-}H}$ = 21.9 Hz, 1H, H1), 8.59 (s, 1H, H3), 7.80 (s, 1H, H5), 7.44 (s, 1H, H6), 7.24 (s, 1H, H8), 7.10 (s, 1H, H10), 5.33 (s, 1H, H12), 1.18-2.16 ppm (m, 16H, C_8H_{16}), 6.54-7.87 ppm (m, 45H, other aromatic protons). ^{31}P NMR (242.9 MHz, CD_2Cl_2): δ = 9.40 (t, $J_{P\text{-}P}$ = 5.8 Hz, $CPPh_3$), -10.53 (dd, $J_{P\text{-}P}$ = 253.4 Hz, $J_{P\text{-}P}$ = 5.8 Hz, $OsPPh_3$), -13.92 (dd, $J_{P\text{-}P}$ = 253.4 Hz, $J_{P\text{-}P}$ = 5.8 Hz, $OsPPh_3$). ^{13}C{^{1}H} NMR plus DEPT-135, ^{1}H-^{13}C HMBC and ^{1}H-^{13}C HSQC (150.9 MHz, CD_2Cl_2): δ = 234.3 (t, $J_{P\text{-}C}$ = 7.25 Hz, C7), 221.4 (t, C11), 201.4 (dt, $J_{P\text{-}C}$ = 25.4 Hz, $J_{P\text{-}C}$ = 5.3 Hz, C4), 200.2 (br, C1), 164.3

(s, C9), 162.1 (s, C6), 159.0 (s, C5), 135.3 (d, $J_{P\text{-}C}$ = 25.1 Hz, C3), 131.9 (dt, $J_{P\text{-}C}$ = 58.1 Hz, $J_{P\text{-}C}$ = 5.4 Hz, C2), 128.9 (s, C8), 114.0 (s, C10), 11.5 (s, C12), 15.1-62.5 ppm (m, C_8H_{16}), 135.0-120.9 ppm (m, other aromatic carbons). HRMS (ESI): m/z calcd for $[C_{74}H_{70}OsP_3O_2]^+$, 1275.41980; found: 1275.41919. Anal. Calcd (%) for $C_{74}H_{70}OsP_3O_2BF_4$: C 65.29, H 5.18; found: C 65.12, H 5.20.

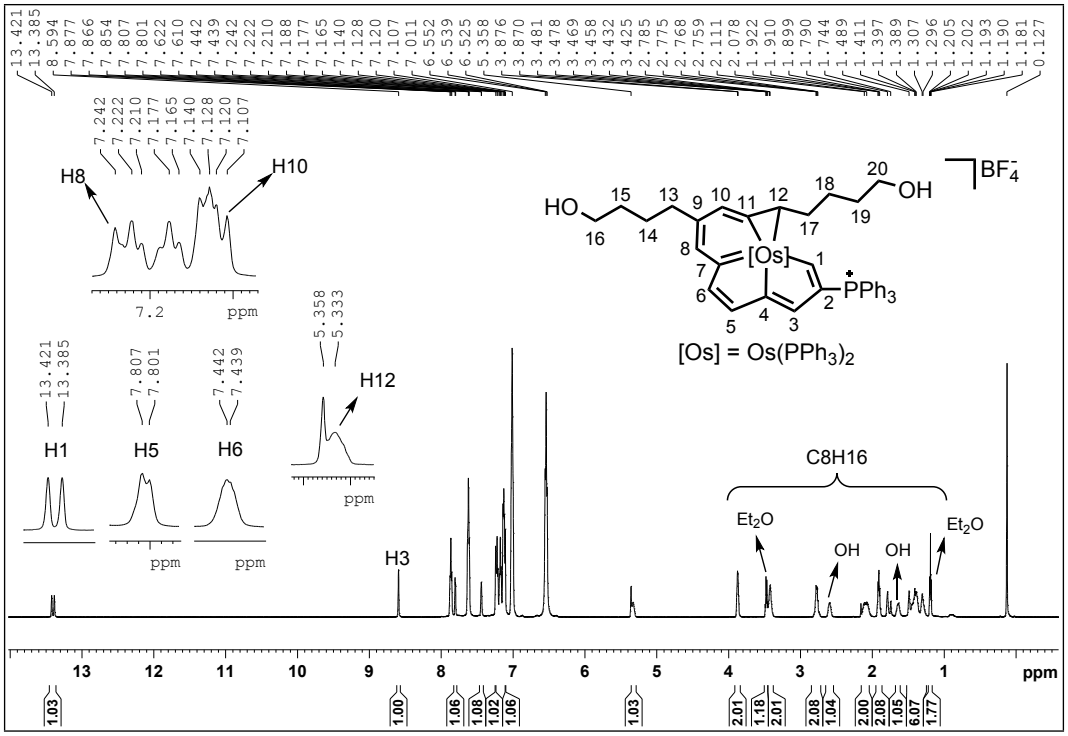

Fig. S1 ^{1}H NMR spectrum (600.1 MHz) of complex **2** in CD_2Cl_2 at room temperature.

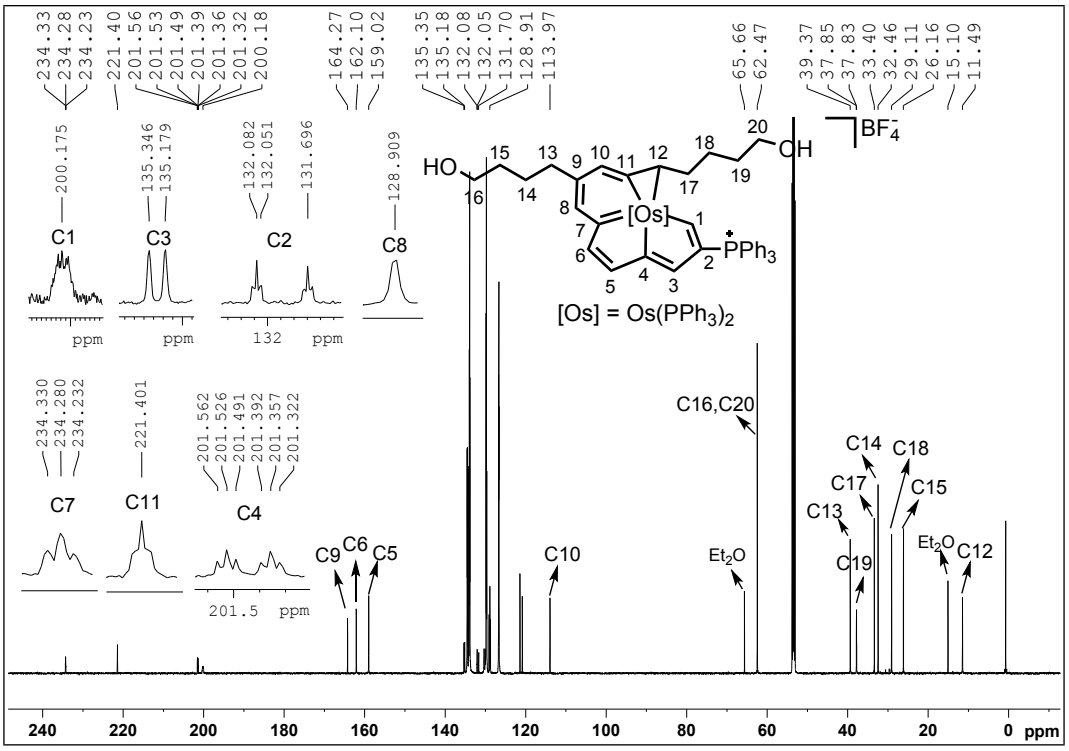

Fig. S2 ^{13}C NMR spectrum (150.9 MHz) of complex **2** in CD_2Cl_2 at room temperature.

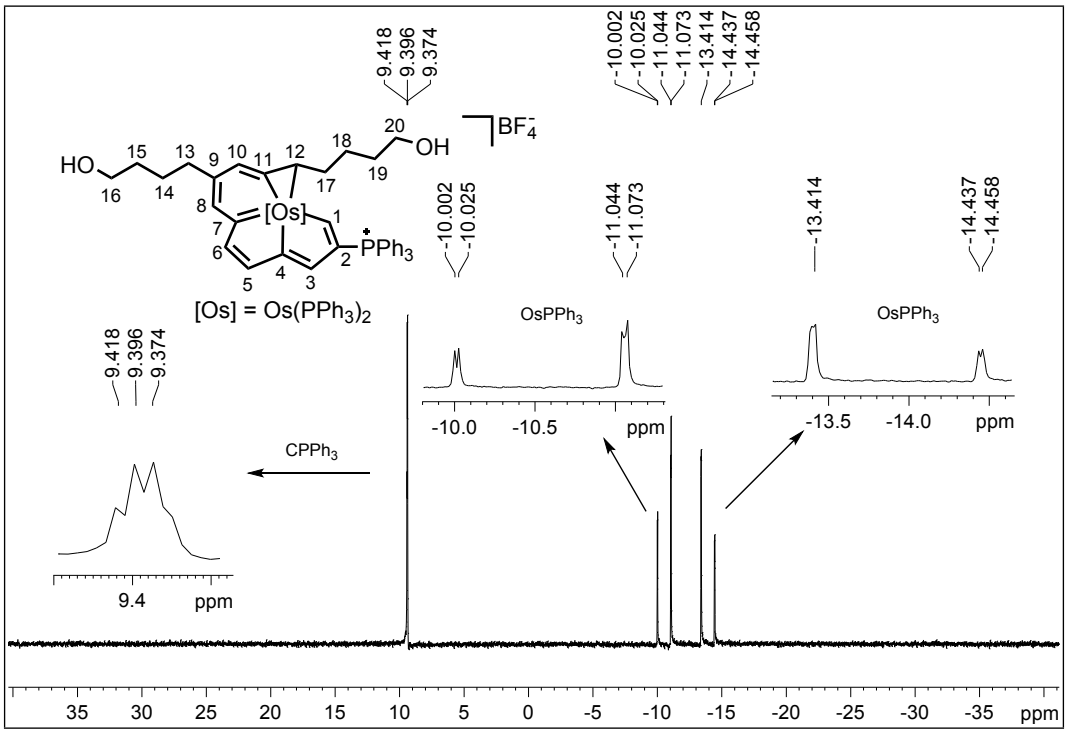

Fig. S3 ^{31}P NMR spectrum (242.9 MHz) of complex **2** in CD_2Cl_2 at room temperature.

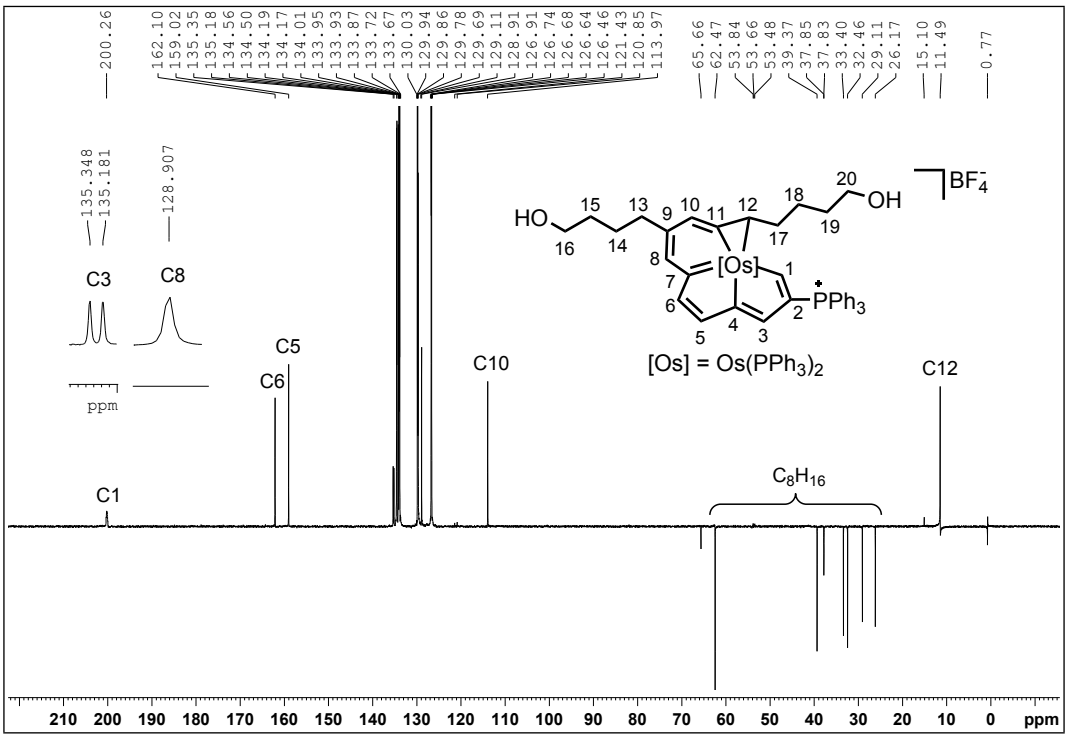

Fig. S4 DEPT-135 spectrum (150.9 MHz) of complex **2** in CD_2Cl_2 at room temperature.

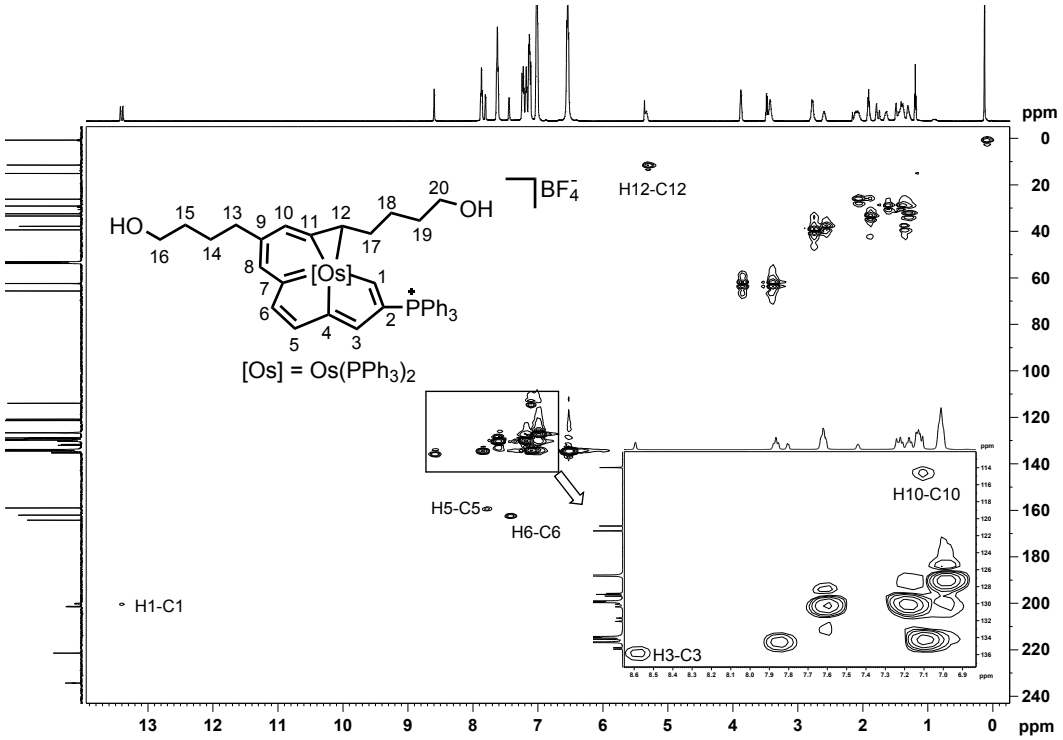

Fig. S5 Two-dimensional ^{1}H-^{13}C HSQC spectrum of complex 2a in CD_2Cl_2 at room temperature.

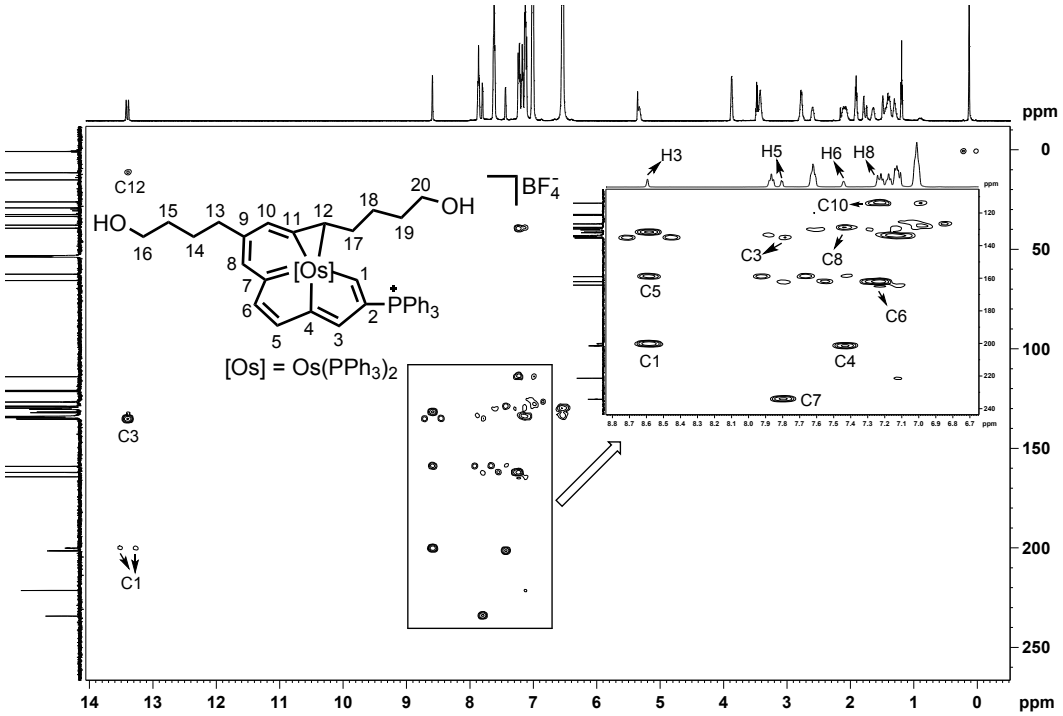

Fig. S6 Two-dimensional ^{1}H-^{13}C HMBC spectrum of complex 2a in CD_2Cl_2 at room temperature.

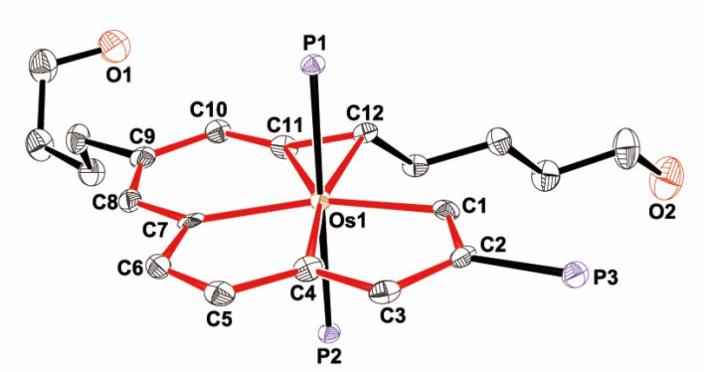

Fig. S7 The X-ray molecular structure for the cation of complex 2.

The phenyl rings of the PPh_3 ligands have been omitted for clarity. Thermal ellipsoids of the remaining non-hydrogen atoms are drawn at 50% probability. Selected bond distances (Å) and angles (deg): Os1–C1 2.103(4), Os1−C4 2.110(4), Os1−C7 2.105(4), Os1−C11 2.039(4), Os1−C12 2.238(4), C1−C2 1.390(6), C2−C3 1.433(6), C3−C4 1.373(6), C4−C5 1.413(6), C5−C6 1.367(6), C6−C7 1.437(6), C7−C8 1.418(6), C8−C9 1.373(6), C9−C10 1.425(6), C10−C11 1.353(6), C11−C12 1.396(6), Os1−C1−C2 116.7(3), C1−C2−C3 115.9(4), C2−C3−C4 113.0(4), C3−C4−Os1 118.8(3), C4−Os1−C1 75.5(16), Os1–C4–C5 117.0(3), C4–C5–C6 114.6(4), C5–C6–C7 117.0(4), C6–C7–Os1 115.0(3), C7–Os1–C4 76.4(16), Os1–C7–C8 130.9(3), C7–C8–C9 126.1(4), C8–C9–C10 121.4(4), C9–C10–C11 122.2(4), C10–C11–Os1

138.3(3), C11–Os1–C7 80.7(17), Os1–C11–C12 78.9(3), C11–C12–Os1 63.4(2), C12–Os1–C11 37.7 (16). The data in the CIF file correspond to the structure of **2**.

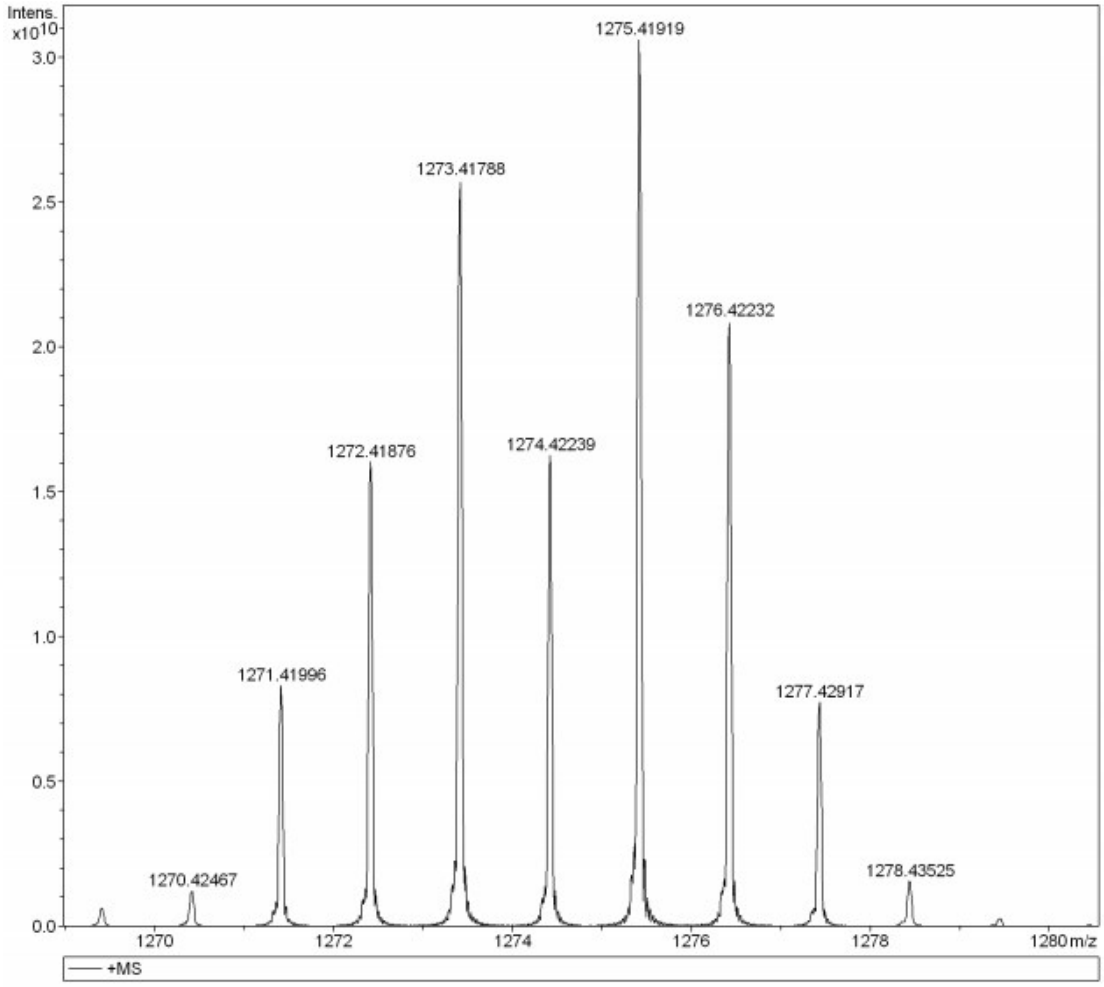

Fig. S8 Positive-ion ESI-MS spectrum of [**2**] $^{+}$ $[C_{74}H_{70}O_2OsP_3]^{+}$ measured in CH_3OH.

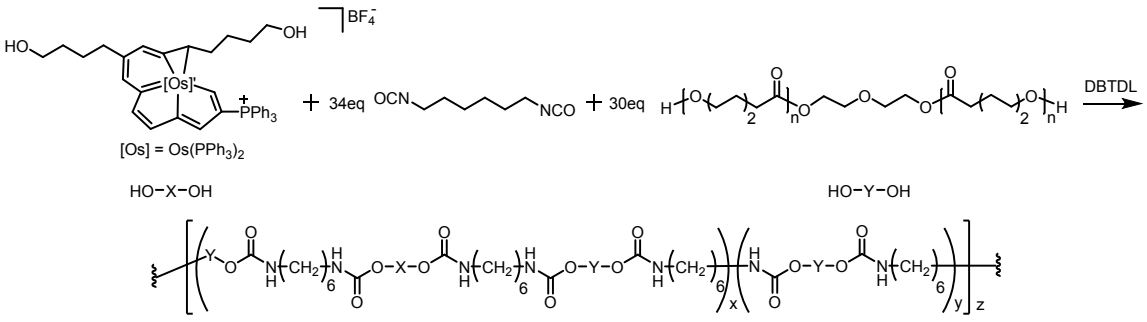

Carbolong Polyurethanes. For a typical polyurethane reaction, **2**, 1,6-diisocyanatohexane (911 μL, 5.67 mmol), dry PCL (M_n = 2000 g mol^{-1}, 10 g, 5 mmol), and dibutyltin dilaurate (DBTDL, 5 μL) were mixed with 50 mL of DMF in a 100 mL flask. N_2 was pumped into the flask three

times to get rid of the oxygen. The mixture reacted at 50 °C for 12 h to yield polyurethane. The polymer was then precipitated twice by methanol to remove oligomers and unreacted reagents. We systematically varied the initial content of **2** (0 – 0.5 wt%) in the reaction mixture and the accurate value in final CLPUs was determined by UV-vis spectroscopy against a standard curve.

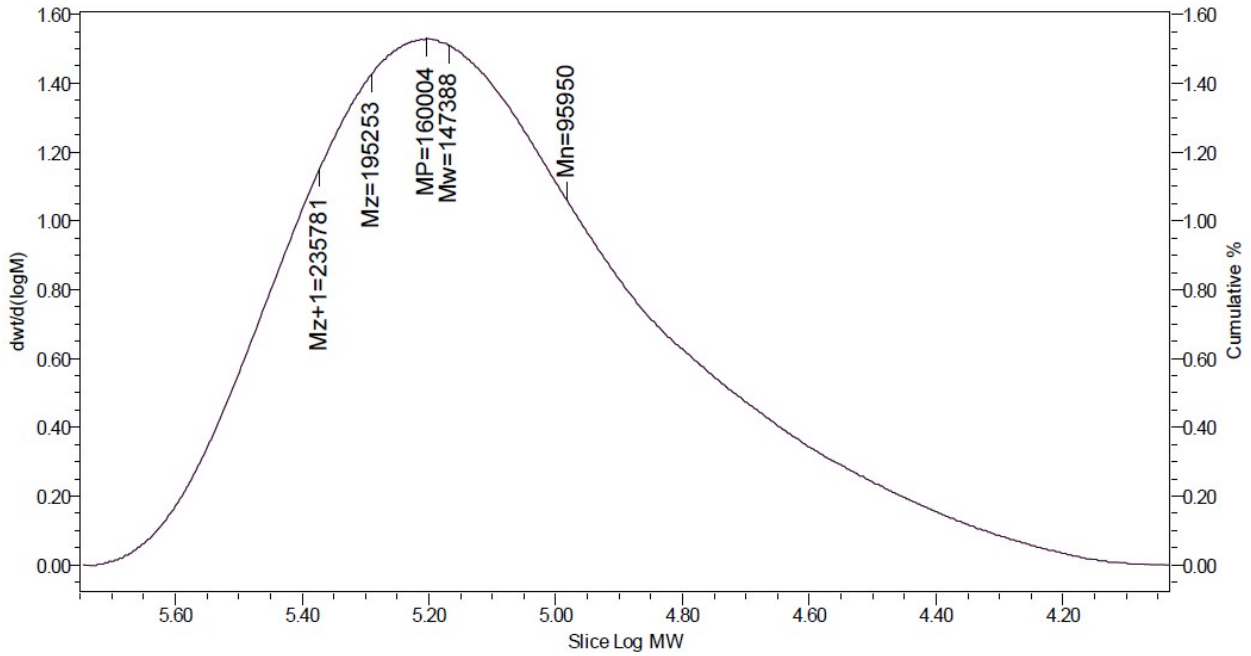

Fig. S9 GPC trace of **CLPU0** (RI signal).

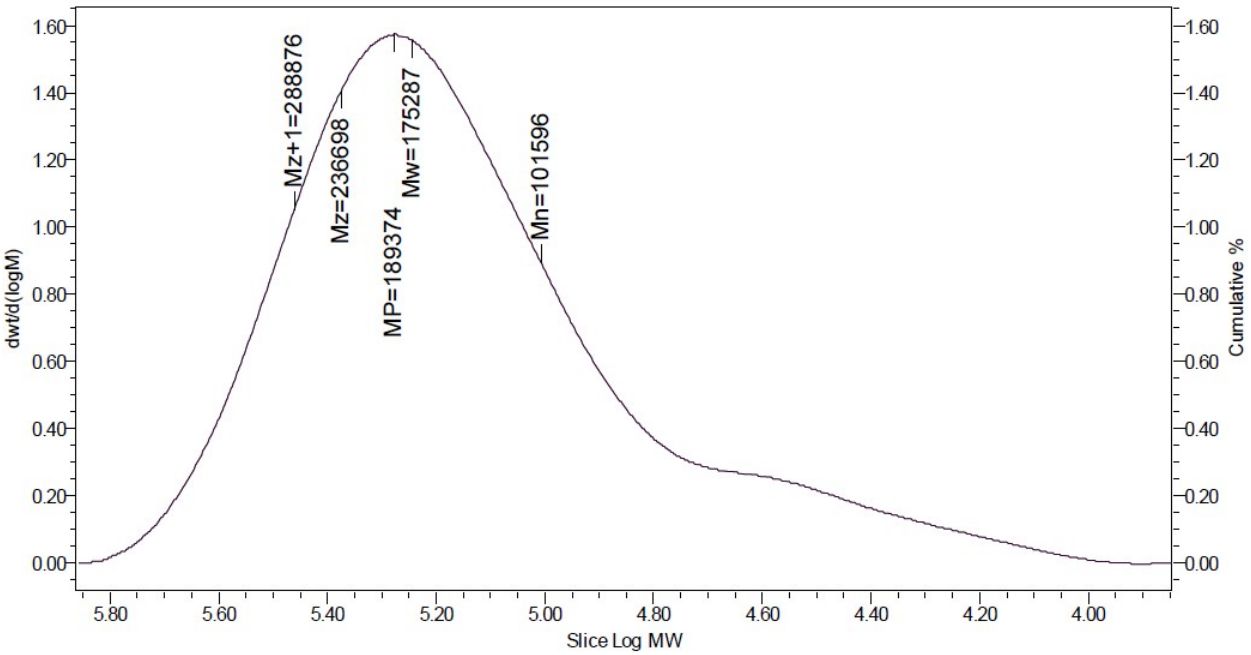

Fig. S10 GPC trace of **CLPU7** (RI signal).

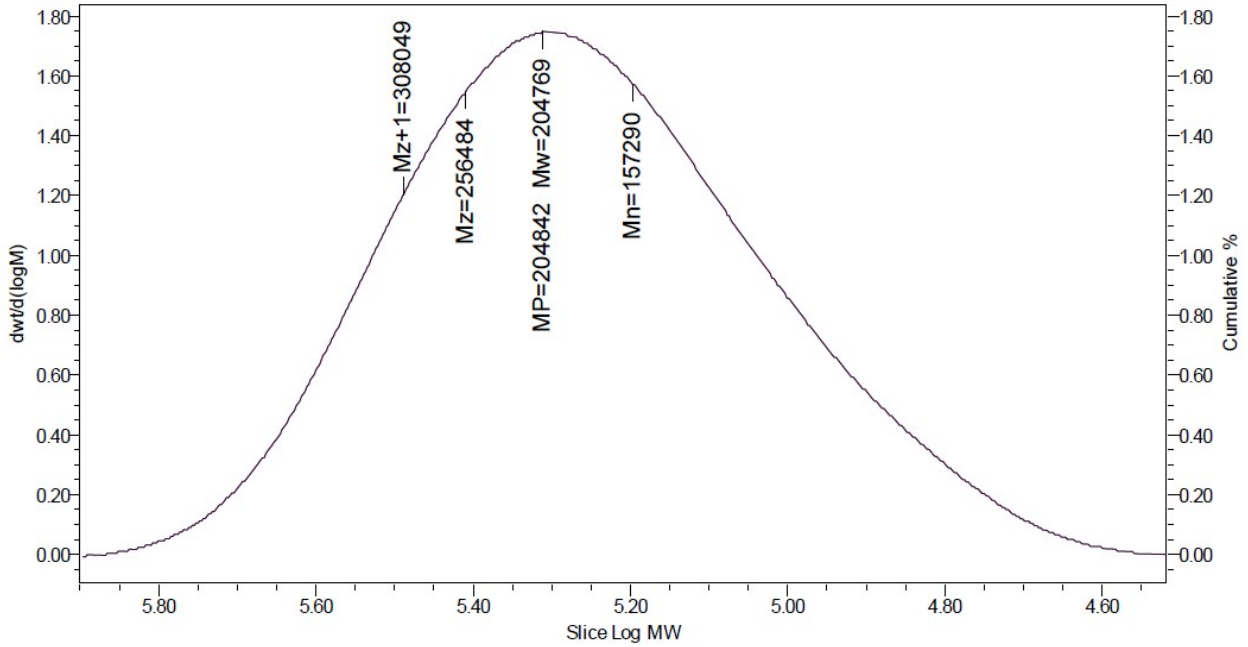

Fig. S11 GPC trace of **CLPU10** (RI signal).

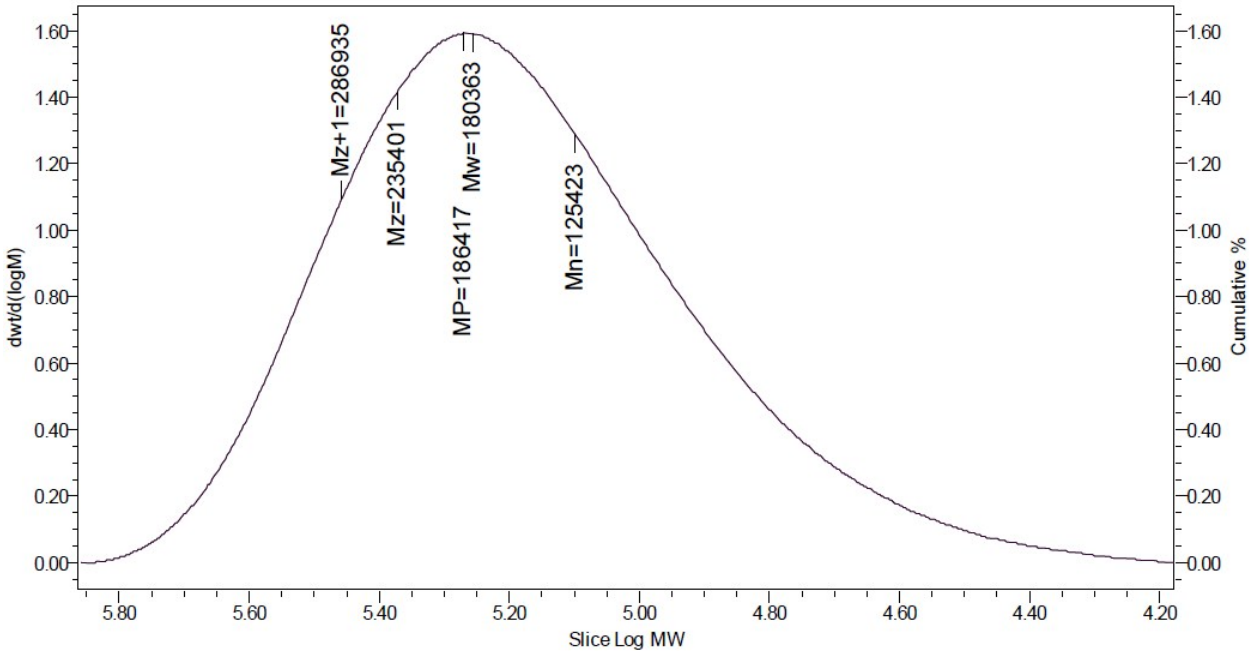

Fig. S12 GPC trace of **CLPU15** (RI signal).

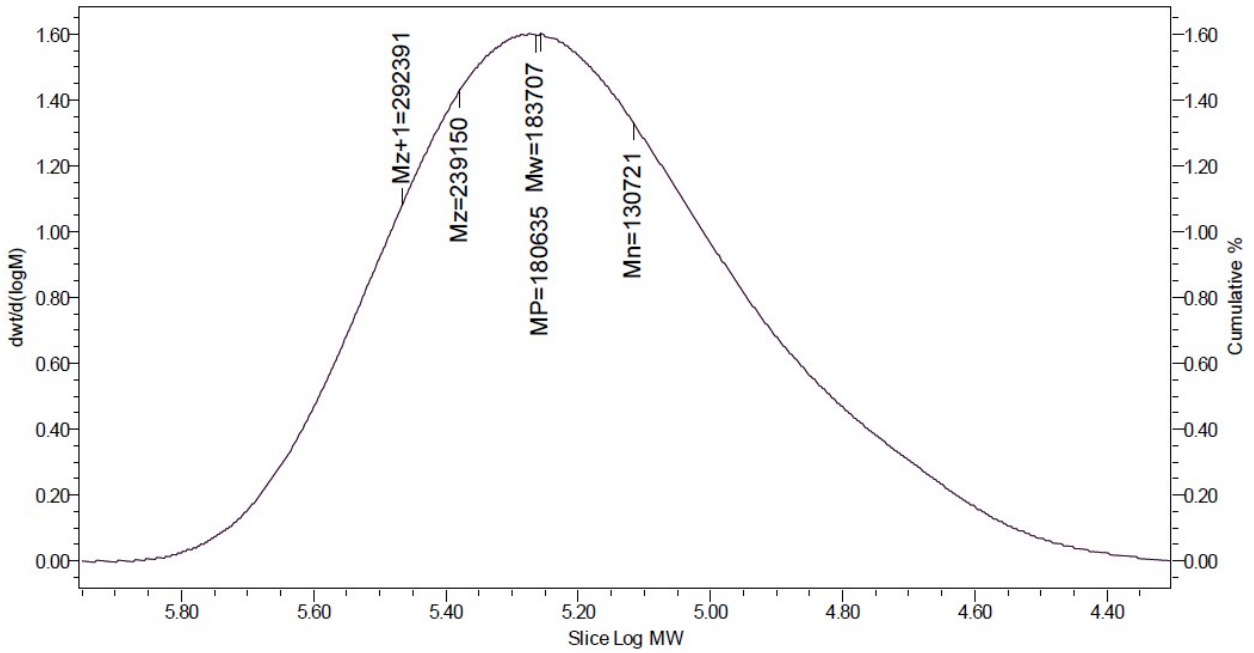

Fig. S13 GPC trace of **CLPU20** (RI signal).

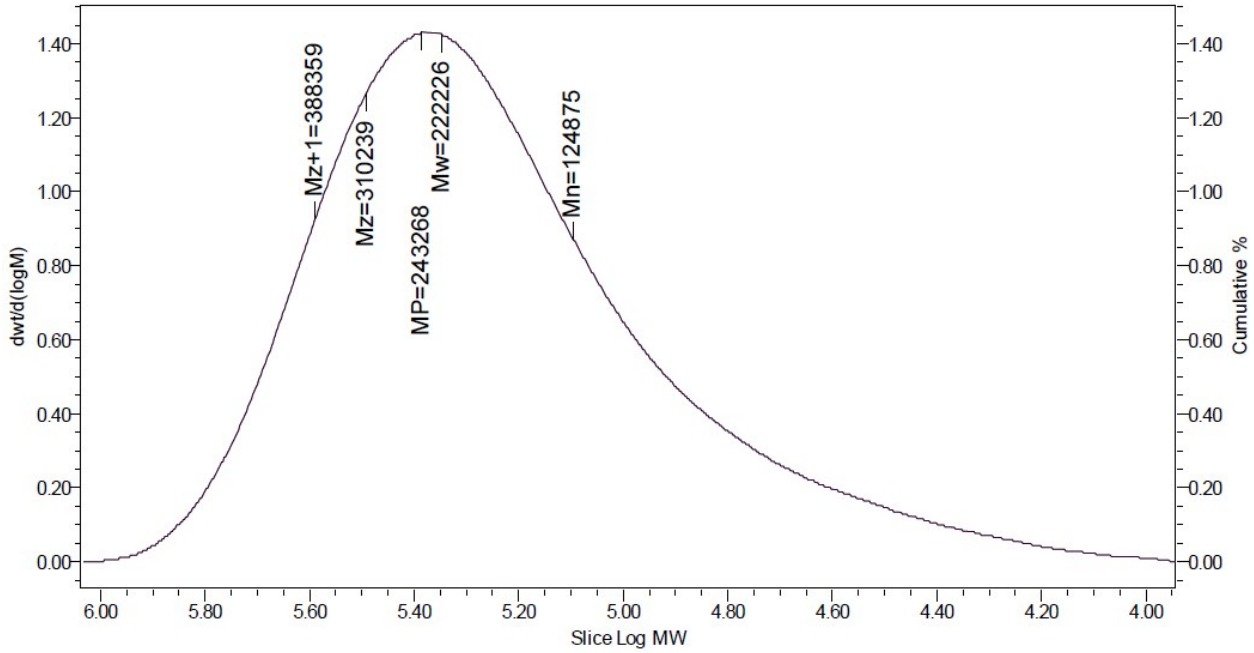

Fig. S14 GPC trace of **CLPU30** (RI signal).

Standard Curve

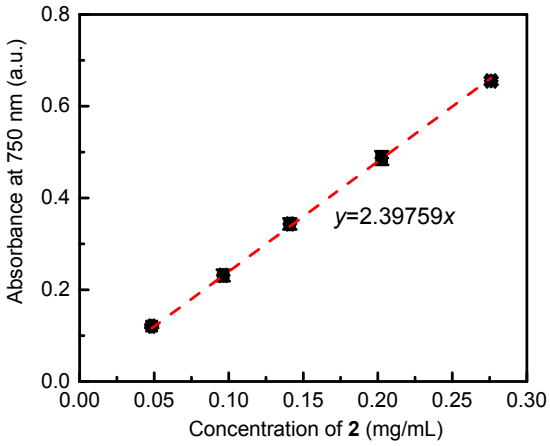

Fig. S15 Standard curve of the absorbance at 750 nm as a function of the concentration of **2** in DMF.

Microstructure

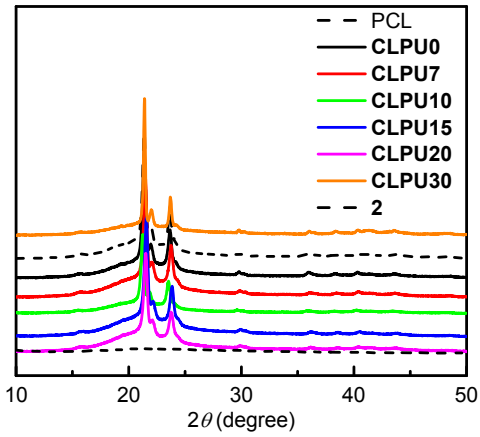

Fig. S16 XRD of PCL, complex **2** and CLPU films at room temperature.

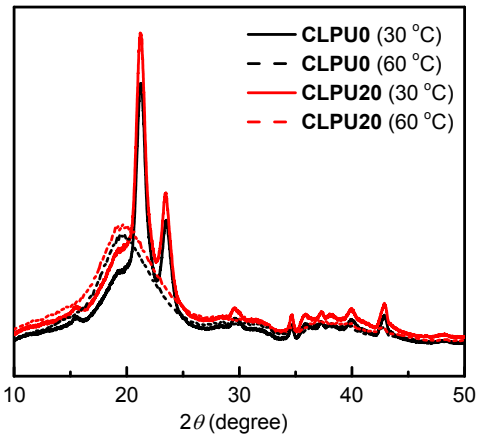

Fig. S17 XRD of **CLPU0** and **CLPU20** at given temperature indicated in the legend.

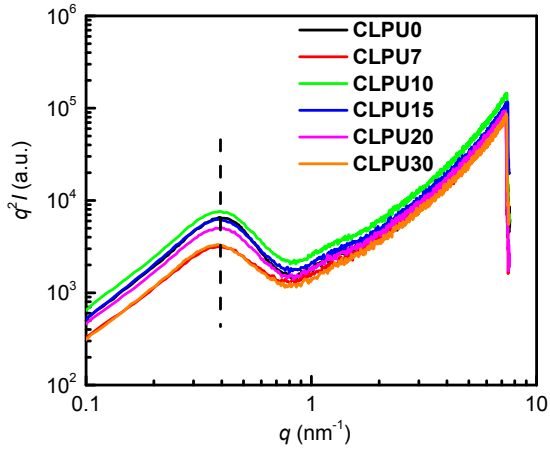

Fig. S18 Lorentz corrected scattering intensity of CLPU films at room temperature. The vertical dashed line indicates the peak.

A primary peak centered at q^*= 0.40 nm^{-1} can be recognized on the Lorentz corrected plot. The corresponding length is 2pi/ q^* = 15.7 nm which corresponds to the interlamellar distance of PCL crystallite.

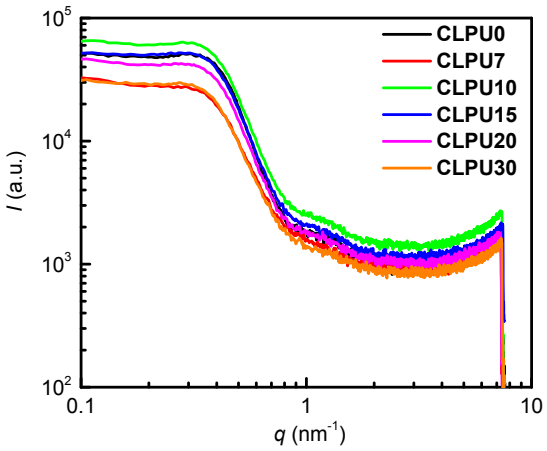

Fig. S19 Scattering intensity of CLPU films at room temperature.

Mechanical Properties

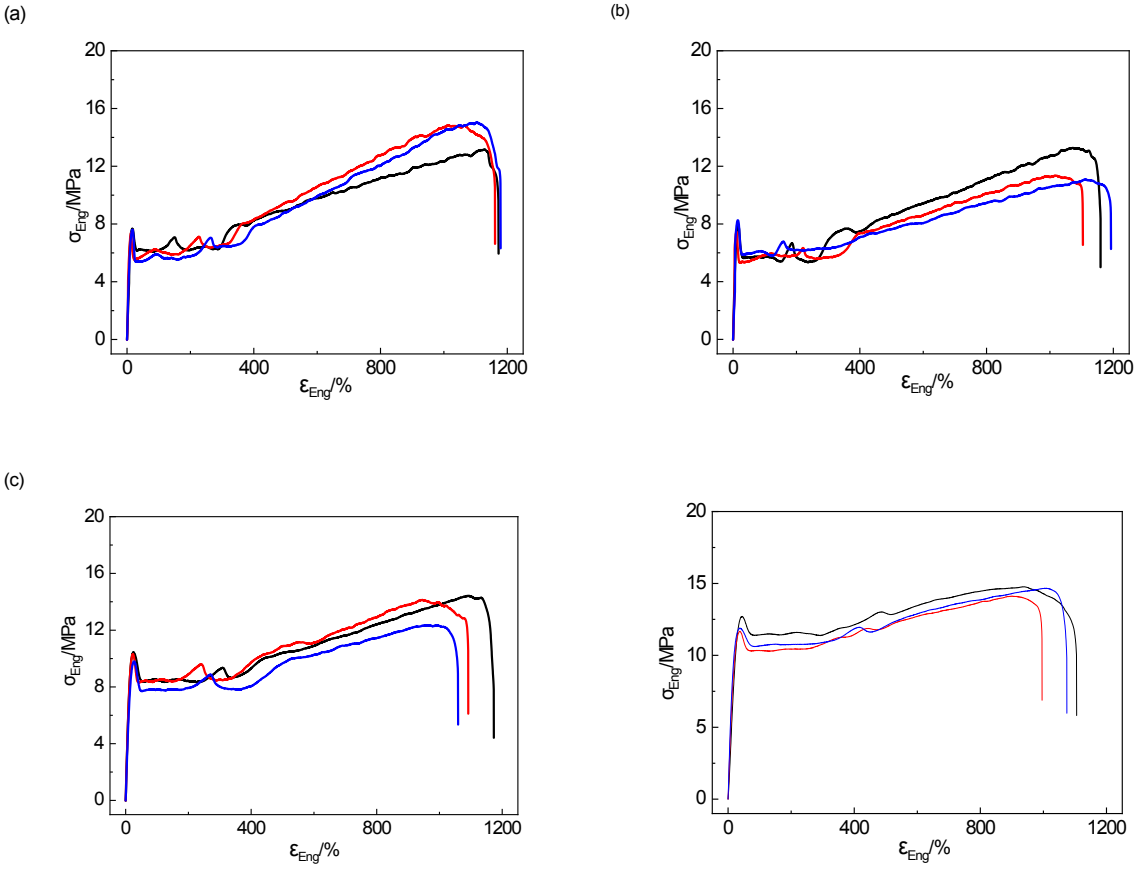

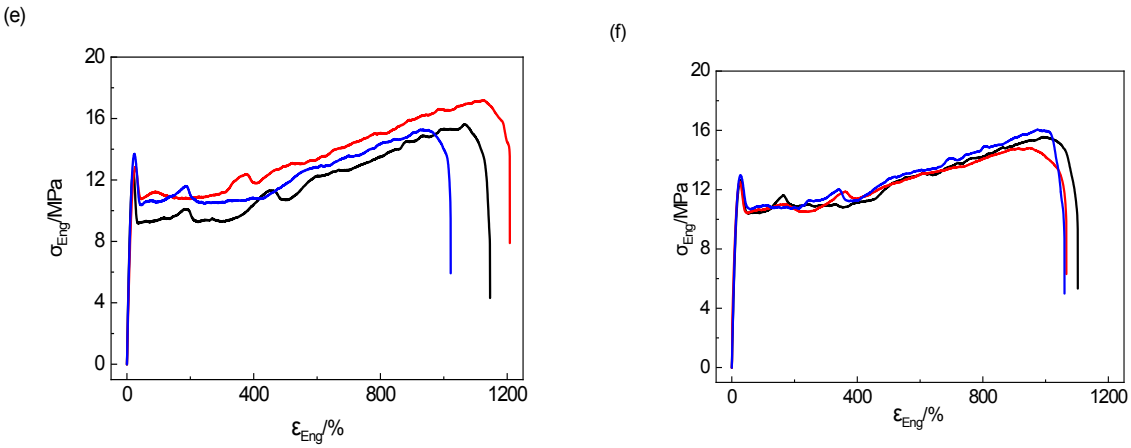

Fig. S20 Stress-strain curves of pristine CLPU films: (a) **CLPU0**, (b) **CLPU7**, (c) **CLPU10**, (d) **CLPU15**, (e) **CLPU20** and (f) **CLPU30**. For each material, three-independent tensile tests were performed.

Photothermal Properties

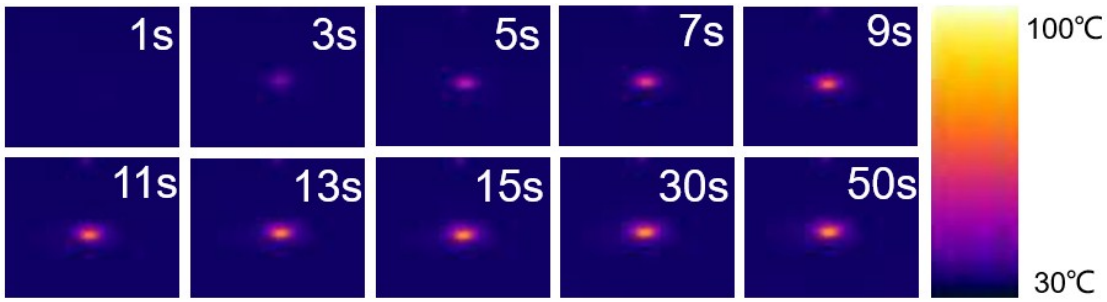

Fig. S21 Thermographic images of **CLPU20** under NIR light (λ = 808 nm, 0.5 W cm^{-2}) at given times. All the thermographic images are in the same scale range.

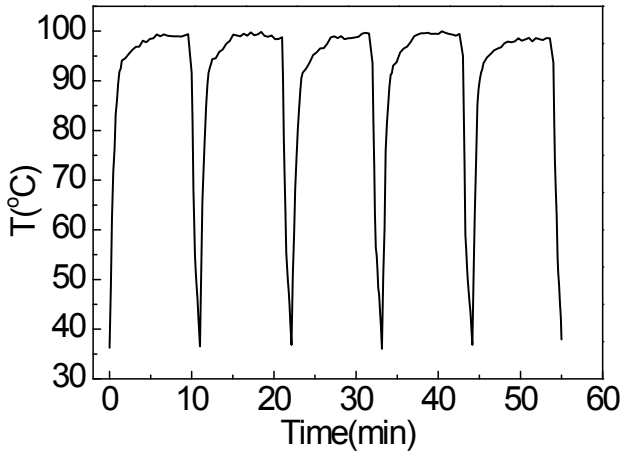

Fig. S22 Temperature variation of **CLPU20** under ON/OFF NIR irradiation (0.5 W cm^{-2}) for 5 cycles.

Light-Induced Healing

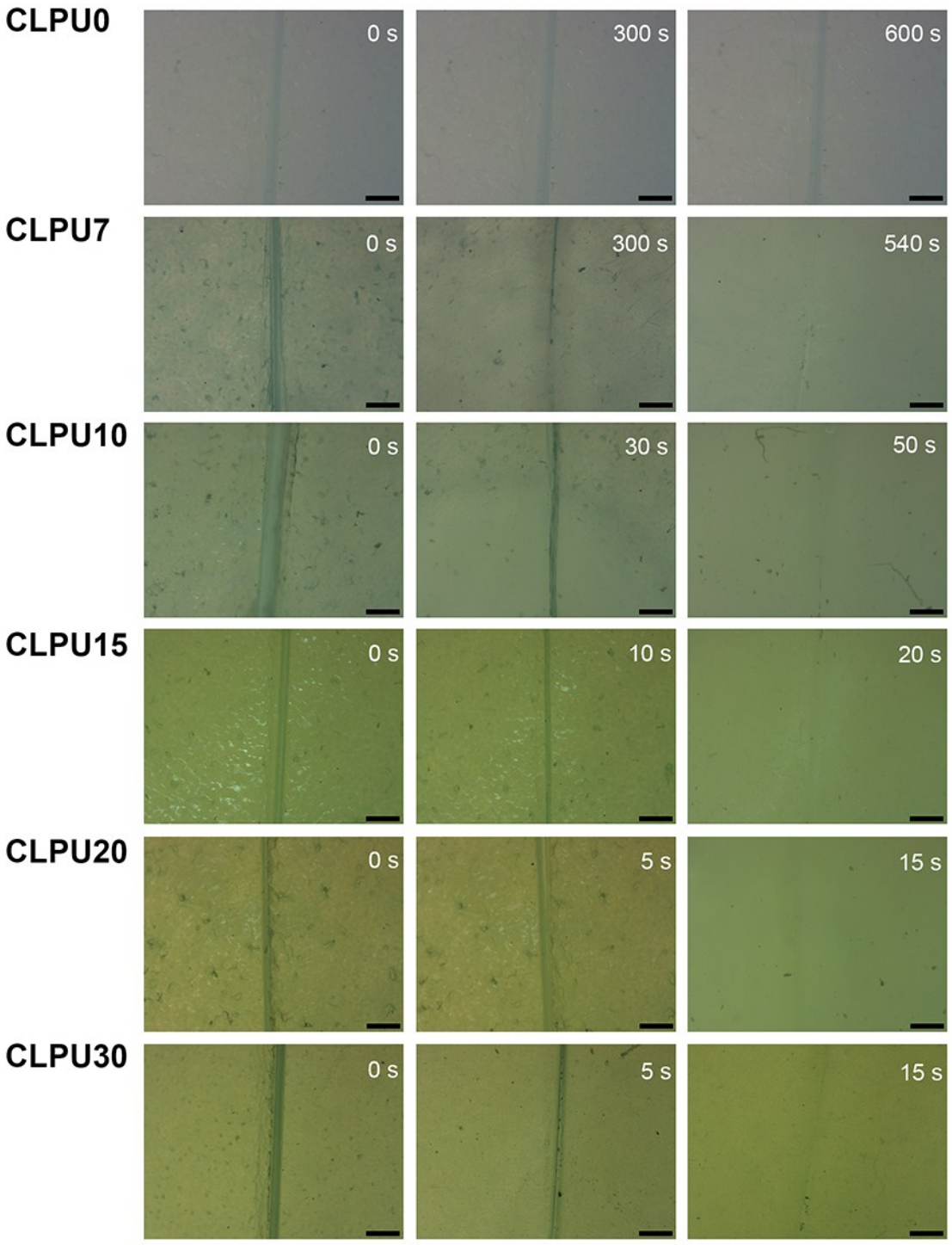

Fig. S23 Optical images of healing process for **CLPU0**, **CLPU7**, **CLPU10**, **CLPU15**, **CLPU20** and **CLPU30** after NIR irradiation (λ = 808 nm, 0.5 W cm^{-2}). The numbers indicate the irradiation time.

(a)

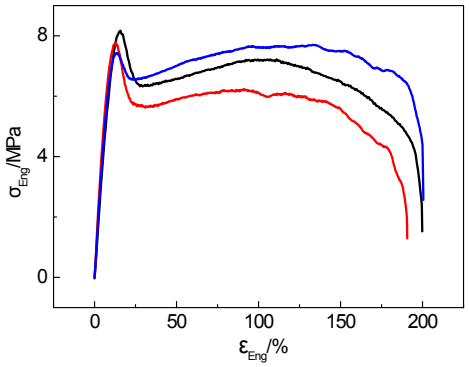
σEng/MPa
εEng/%
0
4
8
0
50
100
150
200

(b)

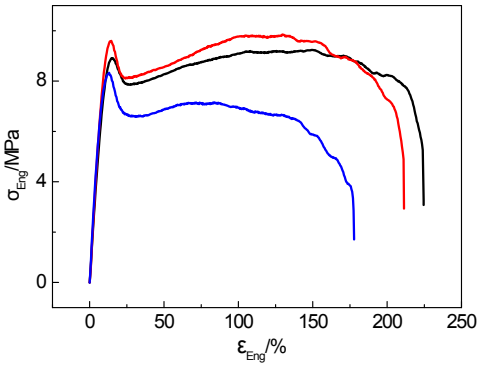
σEng/MPa
εEng/%
0
4
8
0
50
100
150
200
250

(c)

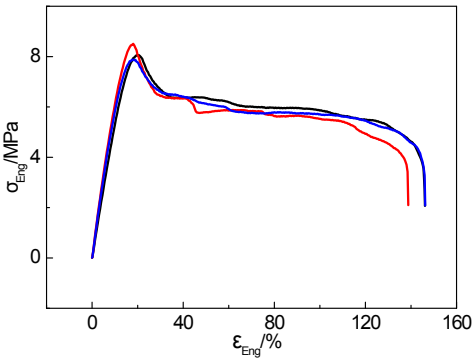
σEng/MPa
εEng/%
0
4
8
0
40
80
120
160

(d)

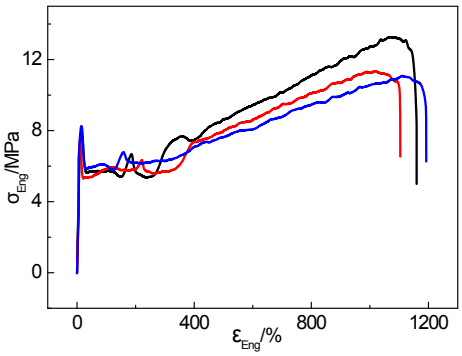
σEng/MPa
εEng/%
0
4
8
12
0
400
800
1200

(e)

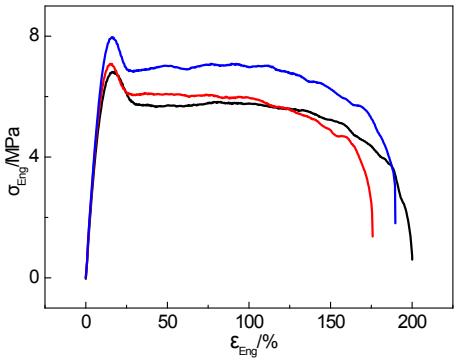
σEng/MPa
εEng/%
0
4
8
0
50
100
150
200

(f)

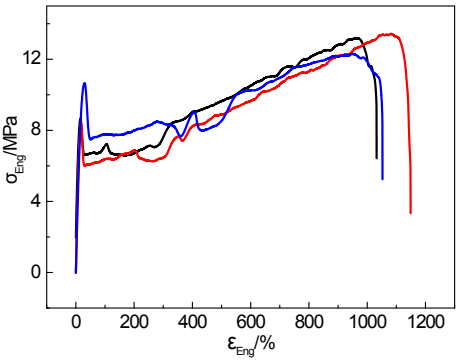
σEng/MPa
εEng/%
0
4
8
12
0
200
400
600
800
1000
1200

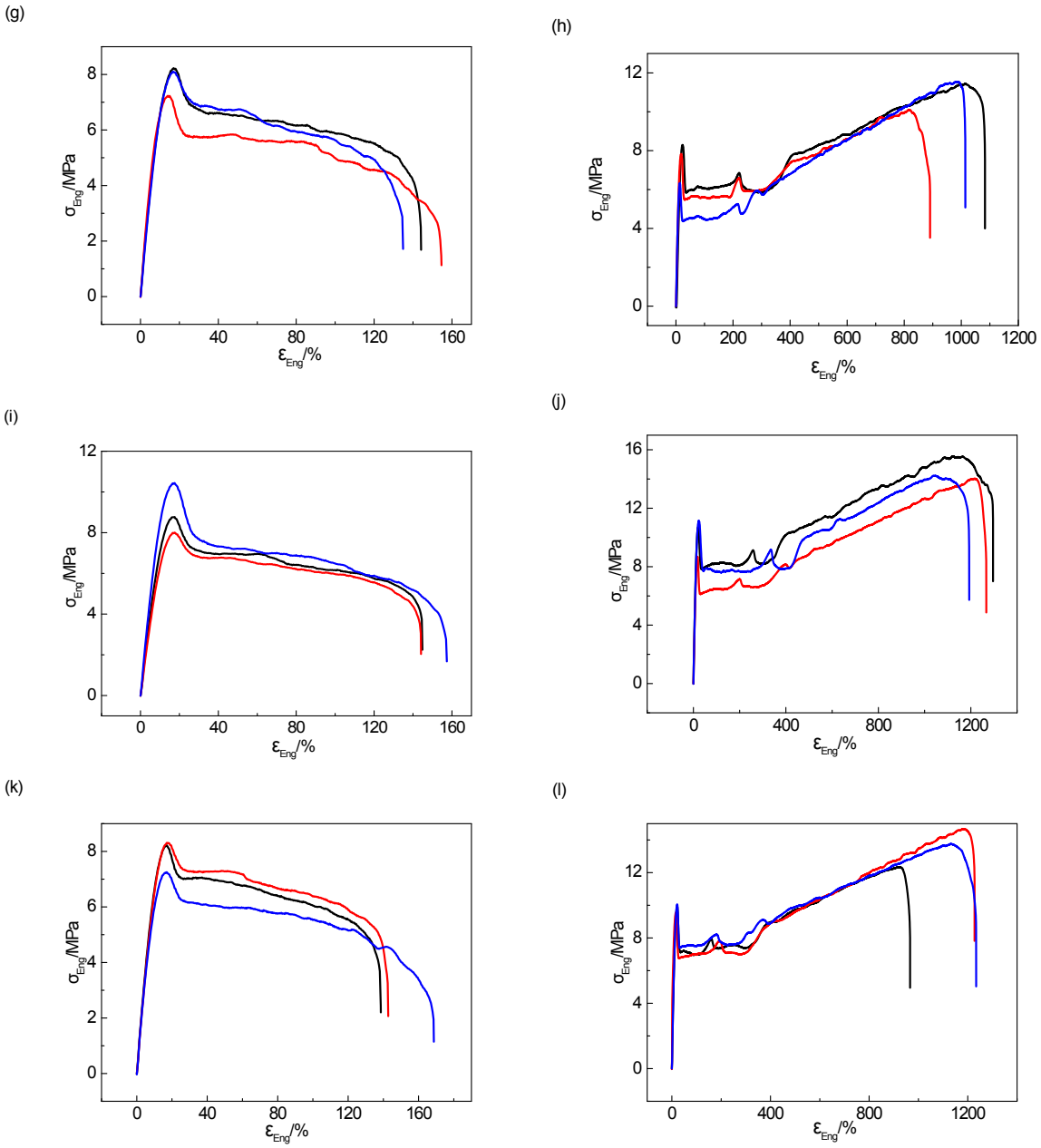

Fig. S24 Stress-strain curves of damaged and healed CLPU films. **CLPU0**: (a) notched and (b) healed; **CLPU7**: (c) notched and (d) healed; **CLPU10**: (e) notched and (f) healed; **CLPU15**: (g) notched and (h) healed; **CLPU20**: (i) notched and (j) healed; **CLPU30**: (k) notched and (l) healed. Three-independent tensile tests were performed for each material, either damaged or healed.

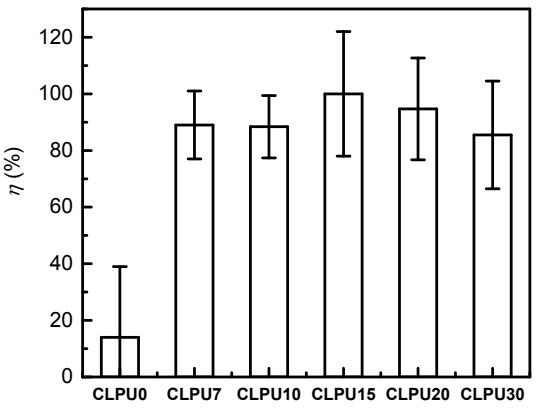

Fig. S25 Healing efficiency for CLPU films. The irradiation times are: 600 s (**CLPU0**), 540 s (**CLPU7**), 50 s (**CLPU10**), 30 s (**CLPU15**), 15 s (**CLPU20**), and 15 s (**CLPU30**).

After NIR irradiation, **CLPU0** showed no healing. Restoration of mechanical properties were seen in the rest of the CLPU samples.

Table S1 Crystal data and structure refinement for complex **2**.

	2·3CH_2Cl_2
empirical formula	$[C_{74}H_{70}O_2OsP_3]BF_4 \cdot 3CH_2Cl_2$
formula weight	1615.99
temperature, K	100.00(10)
crystal system	monoclinic
space group	P21/n
a, Å	12.19810(10)
b, Å	26.75170(10)
c, Å	21.82430(10)
α, °	90
β, °	98.0260(10)
γ, °	90
V, Å^3	7051.95(7)
Z	4
*d*calcd, g cm-3	1.522
μ(CuKα), mm-1	6.619
F(000)	3272.0
crystal size, mm	0.4 × 0.1 × 0.1
2θ range, °	7.774 to 129.994
reflns collected	51957
indep reflns	11985
data/restraints/params	11985/6/849
goodness-of-fit on F^2	1.038
final *R* ($I > 2\sigma(I)$)	R1 = 0.0442 wR2 = 0.1205
R indices (all data)	R1 = 0.0461 wR2 = 0.1224
Residual electron density (e. Å^{-3}) max/min	2.15/-2.03

Table S2 The content of **2** and osmium, and GPC data of CLPU.

Entry	Content of **2** (wt%)[a]	Content of Osmium (wt%)	M_n (kDa)	PDI
CLPU0	0.00	0.000	96	1.54
CLPU7	0.07	0.010	102	1.73
CLPU10	0.10	0.015	157	1.30
CLPU15	0.15	0.020	125	1.44
CLPU20	0.20	0.027	130	1.41
CLPU30	0.30	0.040	125	1.78

[a] The content of **2** was determined by UV-vis spectroscopy.

Table S3 Mechanical properties of CLPU films.

Entry	Young's modulus (MPa)	Yield strength (MPa)	Ultimate strength (MPa)	Strain at break (%)	Toughness (MPa)[a]
CLPU0	73 ± 5	7.5 ± 0.1	14.3 ± 1.0	1100 ± 10	115 ± 4
CLPU7	87 ± 7	7.9 ± 0.4	11.9 ± 1.2	1100 ± 40	98 ± 7
CLPU10	74 ± 5	10.2 ± 0.3	13.6 ± 1.1	1000 ± 50	117 ± 12
CLPU15	80 ± 9	12.1 ± 0.6	14.5 ± 0.3	1050 ± 55	130 ± 12
CLPU20	91 ± 7	13.0 ± 0.6	16.0 ± 1.0	1080 ± 90	142 ± 20
CLPU30	91 ± 7	12.7 ± 0.2	15.4 ± 0.6	1000± 20	135 ± 3

[a] The area under the stress-strain curves.

Table S4 Summary of the recovery of mechanical properties of CLPU films after NIR irradiation

Entry		Young's modulus (MPa)	Ultimate strength (MPa)	Yield Strength (MPa)	Strain at break (%)	Toughness (MPa)	η (%)
CLPU0	**pristine**	72 ± 8	14.3 ± 0.9	7.6 ± 0.2	1200 ± 50	115± 4	14 ± 25
	notched	83±10	1.8±0.7	7.8±0.4	200±5	12±2	
	healed	98±7	2.6±0.8	8.9±0.7	200±20	16±4	
CLPU7	**pristine**	87±8	12.5±1.2	8.2±0.2	1200±70	111±11	89 ± 12
	notched	62±6	3.0±0.1	8.1±0.3	150±4	8±1	
	healed	102 ± 22	11.8 ± 1.2	7.9 ± 0.4	1100± 50	99± 8	
CLPU10	**pristine**	74 ± 5	13.6 ± 1.1	10.2 ± 0.3	1000 ± 50	117 ± 12	88 ± 11
	notched	68 ± 2	1.3 ±0.6	7.3 ±0.6	190 ±10	10 ± 1	
	healed	76 ± 16	13.0 ± 0.6	9.2 ±1.2	1000 ± 73	103 ± 4	
CLPU15	**pristine**	80 ±1	11.7 ± 1.2	11.0 ± 1.0	750 ± 90	78 ± 13	100 ± 22
	notched	74 ± 3	1.5 ±0.3	7.8 ±0.5	140 ±10	8 ± 1	
	healed	60 ± 10	11.0 ± 0.8	7.5 ±1.0	950 ± 110	78 ± 12	
CLPU20	**pristine**	91 ± 7	16.0 ± 1.0	13.0 ± 0.6	1080 ± 90	142 ± 20	94.7 ± 18
	notched	76 ± 9	2.0 ±0.2	9.0 ±1.2	150 ±7	9 ± 1	
	healed	78 ± 5	14.5 ± 0.9	10.1 ±1.3	1200 ± 30	134 ± 15	
CLPU30	**pristine**	91 ± 7	15.4 ± 0.6	12.7 ± 0.2	1000 ± 20	135 ± 3	85.5 ± 19
	notched	68 ± 3	1.8 ±0.6	7.9 ±0.5	150 ±16	9 ± 1	
	healed	76 ± 7	13.5 ± 1.2	9.8 ±0.2	1100 ± 150	116 ± 22	

Supporting Reference

[1] Zhu, C.; Yang, C.; Wang, Y.; Lin, G.; Yang, Y.; Wang, X.; Zhu, J.; Chen, X.; Lu, X.; Liu, G.; Xia, H. Ccccc Pentadentate Chelates with Planar Möbius Aromaticity and Unique Properties. *Sci. Adv.* **2016,** *2* (8), e1601031.
[2] Stribeck, N., X-Ray Scattering of Soft Matter. In *X-Ray Scattering of Soft Matter*, Pasch, H., Ed. Springer: 2007; pp 117-118.